phys. stat. sol. (b) 67, 609 (1975)

Subject classification: 1.1 and 11

Institute of Atomic Physics, Bucharest

Transfer Matrix Approach to Axial Hyperchanneling

By

A. CORCIOVEI and M. APOSTOL

The mechanism of channeling is reviewed and a discrete model for hyperchanneling is formulated, which holds both for planar and axial channeling. It is assumed that the moving particle in the crystal interacts with the atoms in the planes of the lattice which are perpendicular to its direction of motion. An axial channel consists in a succession of parallel rings of atoms. The interaction between hyperchanneled particle and these atomic rings is described in terms of classical collisions. From the linearized equations of motion in the momentum approximation one obtains that the interaction with the rings can be described by a transfer matrix which relates the mechanical states of the particle before and after a collision with an atomic ring. Then by induction the mechanical state parameters of the particle after the n-th collision are obtained in terms of the initial conditions. Minimum critical hyperchanneling energies are derived. Expressions are given for the critical angles as well as for the energy losses in the case of the f.c.c. ⟨100⟩ channel. Numerical evaluations show a good agreement between the theoretical results and the experiment.

Der Kanalisierungs-Mechanismus wird erneut betrachtet und ein diskretes Modell für Hyperkanalisierung wird vorgeschlagen, das sowohl für planare als auch für axiale Kanalisierung gültig ist. Es wird angenommen, daß das bewegte Teilchen im Kristall mit den Atomen in den Ebenen des Gitters, die senkrecht zu seiner Bewegungsrichtung sind, wechselwirkt. Ein axialer Kanal besteht aus einer Folge von parallelen Ringen von Atomen. Die Wechselwirkung zwischen dem hyperkanalisierten Teilchen und diesen Atomringen wird mit klassischen Stößen beschrieben. Aus den linearisierten Bewegungsgleichungen ergibt sich in der Impulsnäherung, daß die Wechselwirkung mit den Ringen durch eine Transfermatrix beschrieben werden kann, die den mechanischen Zustand des Teilchens vor und nach einem Stoß mit dem atomaren Ring verknüpft. Darauf werden mit den Anfangsbedingungen durch Induktion die mechanischen Zustandsparameter des Teilchens nach dem n-ten Stoß erhalten. Minimale kritische Hyperkanalisierungsenergien werden abgeleitet. Ausdrücke werden sowohl für die kritischen Winkel als auch für die Energieverluste für den Fall des k.f.z. ⟨100⟩ Kanals angegeben. Die numerischen Berechnungen zeigen gute Übereinstimmung zwischen den theoretischen Ergebnissen und dem Experiment.

1. Introduction

Channeled trajectories of fast charged particles in crystal lattices were discovered in 1961 by Robinson and Oen's machine calculations [1] and analytically described in the special case of the motion near the axis of the channel by Lehmann and Leibfried [2]. Subsequently, Lindhard has given a comprehensive treatment of the directional effects in crystals [3], assuming a classical picture of the particle trajectories. The particle motion proceeds by successive binary encounters with the individual target atoms. Since the deflection angles are small the trajectory of a channeled particle is very nearly a straight line. Therefore, the particle spends most of its time close to the atomic rows which are parallel to this straight line. Lindhard proves that successive binary encounters with the atoms of such a row or a parallel plane can be approximated by an

equivalent action of continuum row or planar potentials (continuum approximation). The energy loss due to the collisions with the target atoms is a negligibile second-order effect, proportional to the square of the deflection angle. Moreover, the transverse energy (the energy of the motion perpendicular to the channeling direction) is assumed to be conserved. At close encounters (large deflection angles) the continuum approximation breaks down and, then, the concept of conservation of transverse energy is not applicable. This breakdown gives a measure of the critical minimum distance of approach and from that the critical angle is derived.

The present paper is also devoted to the description of the particle motion through the crystal as a succession of binary classical collisions with the crystal atoms. However, the discrete structure of the lattice is involved here by means of the interaction with the atoms in the lattice planes which the particle traverses ("rings of atoms", see below) and not by groups of atoms along the motion of the projectile as atomic rows or planes. This is the main difference between the present approach and Lindhard's one. Thus in Lindhard's case the groups of atoms are along the motion of projectile, while in the present paper the groups are in the planes transverse to the projectile motion. A particle moving along a certain crystalline direction is properly axially channeled if it oscillates around the channel axis without escaping from the channel. These particles form the special class of the hyperchanneled particles, characterized by a smaller energy loss and critical angle in comparison with the ordinary channeled particles [4, 5]. We are dealing in the following with hyperchanneled particles.

The particle motion in a channel proceeds by individual collisions with the atoms of that channel. The channel is assumed to be formed by a periodic succesion of parallel rings, whose shape depends upon the orientation of the channel. For simplicity we consider only circular rings. Their centres coincide with the channel axis. The potential sources are distributed on each ring and described by the density function $\varrho(\theta)$, where θ is the position angle of a point on the ring. First we allow an arbitrary function of θ. To introduce the real structure of the channel[1]) we replace, finally, $\varrho(\theta)$ by a number of delta functions according to the atomic location of the potentials. Thus, for the channel shown in Fig. 1 (e.g. f.c.c. $\langle 100 \rangle$) which will be considered as an illustration of our approach, the potential source density will be taken as

$$\varrho(\theta) \sim \delta(\theta) + \delta(\theta - \pi)$$

and

$$\varrho(\theta) \sim \delta\left(\theta - \frac{\pi}{2}\right) + \delta\left(\theta - \frac{3\pi}{2}\right)$$

(respectively, see Section 2).

[1]) There is a special case when the rings are not useful, namely, when the atoms around a channel are concentrated near the ends of parallel diameters, one diameter for each ring. The plane generated by this family of diameters is the plane in which the channeled particle moves. Indeed, in order to penetrate along this channel a particle can only have a very small amplitude of oscillation in the direction perpendicular to this plane as compared to the direction parallel to the plane. The motion then is, mainly, two-dimensional in the above mentioned plane. Along such a planar channeling direction the interaction of the particle with the successive perpendicular planes of atoms varies periodically and it can be approximated by a periodic succession of average (effective) potentials [6, 7].

Fig. 1. The f.c.c. ⟨100⟩ channel

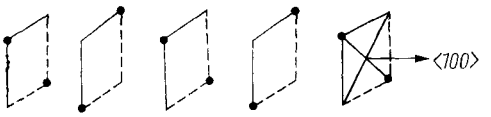

We leave out surface effects and electronic stopping. The particle trajectory considered is due to a sequence of binary interactions between target atoms and the projectile based on classical collisions. The deflection angles are imposed to be small. In the present paper we restrict to a linearization of the equations of the motion in the momentum approximation. The trajectory of the particle through the channel can then be described by a transfer matrix. The usual manner of applying the transfer matrix technique leads us to put into evidence minimum critical hyperchanneling energies. Hyperchanneling critical angles are derived by requiring the particle not to leave the channel. The temperature dependence of these critical angles is also taken into account. The ranges of validity of the linearization approximation is also estimated.

The mathematical model and the transfer matrix technique are developed in Section 2. Some numerical evaluations and conclusions are presented in Section 3.

2. The Hyperchanneling Model

In Fig. 2 and 3 a fragment is shown of the particle trajectory and a ring of the axial channel. The radius of the ring is R and the rings are separated by the distance P.[2]) M is the point of the intersection of the nondeviated trajectory $\overline{MM_1}$ with the plane $x0y$ of the ring. The angles α and β characterize the direction of the trajectory after the collision with the previous ring. The axes Mx_1, My_1, Mz_1 are parallel to $0x$, $0y$, $0z$, respectively, 0 being the centre of the ring. The point N is on the ring as is shown in Fig. 3. The position of the particle within the channel is determined by the projections of M on the axes $0x$ and $0y$, x' and y', respectively.

The potential generated by an element $R\mathrm{d}\theta$ of the circumference at the distance s is

$$\mathrm{d}V = \varrho(\theta)\, f(s)\, R\mathrm{d}\theta\,, \tag{2.1}$$

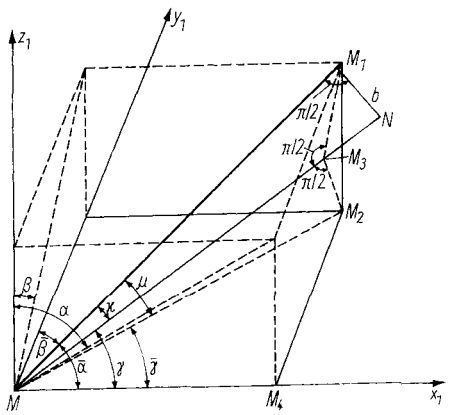

Fig. 2. A fragment of the particle trajectory

[2]) Generally, it is not the periodicity length; for the channel in Fig. 1 the periodicity length is $2P$.

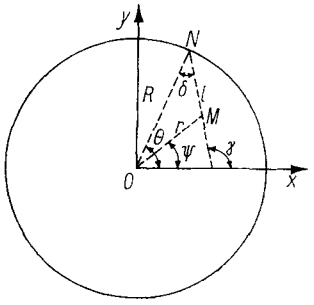

Fig. 3. The plane of the ring with explanations for the angles used in the text

where $\varrho(\theta)$ is the potential source density and $f(s)$ is the potential of the unit source. The deviation angle due to the elementary potential $\mathrm{d}V$ is, in the momentum approximation[3]),

$$\mathrm{d}\Omega = \varrho(\theta)\frac{R\mathrm{d}\theta}{E}\int_1^\infty \frac{\mathrm{d}u}{(u^2-1)^{1/2}}(\operatorname{sgn}\sin\theta)\frac{\mathrm{d}}{\mathrm{d}u}f(|b|\,u)\,, \tag{2.2}$$

where E is the particle energy,

$$\left.\begin{aligned} b &= l\sin\varkappa\,,\\ \cos\varkappa &= \cos\gamma\cos\bar{\alpha}+\sin\gamma\cos\bar{\beta}\,,\\ \gamma &= \theta+\delta\,,\\ \sin\delta &= \frac{r}{l}\sin(\theta-\psi)\,,\\ l &= [R^2+r^2-2Rr\cos(\theta-\psi)]^{1/2}\,,\\ r &= (x'^2+y'^2)^{1/2}\,,\\ \tan\psi &= \frac{y'}{x'}\,, \end{aligned}\right\} \tag{2.3}$$

b is the collision parameter, and the other quantities are shown in Fig. 2 and 3. The factor $\operatorname{sgn}\sin\theta$ in (2.2) is in connection with the existence of $|b|$ in the same relation.

We denote by $\varkappa_x$ the projection of the angle $\varkappa$ on the plane $x0z$ and the relations

$$\cos\mu = \frac{\cos\varkappa}{\cos(\gamma-\bar{\gamma})} = (\cos^2\bar{\alpha}+\cos^2\bar{\beta})^{1/2}\,, \qquad \tan\varkappa_x = \frac{\tan\mu}{\cos\bar{\gamma}} \tag{2.4}$$

easily follow from Fig. 2. By derivation with respect to $\varkappa$ we obtain the projection $\mathrm{d}\Omega_x$ of the angle $\mathrm{d}\Omega$ on the plane $x0z$:

$$\mathrm{d}\Omega_x = \frac{\cos\bar{\alpha}}{\sin^2\bar{\beta}\,(\sin^2\bar{\beta}-\cos^2\bar{\alpha})^{1/2}}\tan\varkappa\,\mathrm{d}\Omega\,. \tag{2.5}$$

[3]) The deviation angle in the momentum approximation and in the laboratory system is given by $\frac{1}{E}\int_1^\infty \frac{\mathrm{d}u}{(u^2-1)^{1/2}}\frac{\mathrm{d}}{\mathrm{d}u}V(bu)$, V being the potential of the source.

The projection $\mathrm{d}\Omega_y$ of the angle $\mathrm{d}\Omega$ on the plane $y0z$ is

$$\mathrm{d}\Omega_y = \frac{\cos\bar{\alpha}}{\cos\bar{\beta}}\,\mathrm{d}\Omega_x\,. \tag{2.5'}$$

The angles after the collision, α' and β' result by adding $\int \mathrm{d}\Omega_x$ and $\int \mathrm{d}\Omega_y$ to α and β, respectively. We obtain

$$\left.\begin{aligned}
\alpha' &= \alpha + \frac{\cos\bar{\alpha}}{\sin^2\bar{\beta}\,(\sin^2\bar{\beta} - \cos^2\bar{\alpha})^{1/2}}\,\frac{R}{E}\int_0^{2\pi}\mathrm{d}\theta\varrho(\theta)\,(\operatorname{sgn}\sin\theta)\times \\
&\quad\times\tan\varkappa\int_1^{\infty}\frac{\mathrm{d}u}{(u^2-1)^{1/2}}\,\frac{\mathrm{d}}{\mathrm{d}u}f(|b|\,u)\,, \\
\beta' &= \beta + \frac{\cos^2\bar{\alpha}}{\cos\bar{\beta}\sin^2\bar{\beta}\,(\sin^2\bar{\beta} - \cos^2\bar{\alpha})^{1/2}}\,\frac{R}{E}\int_0^{2\pi}\mathrm{d}\theta\varrho(\theta)\,(\operatorname{sgn}\sin\theta)\times \\
&\quad\times\tan\varkappa\int_1^{\infty}\frac{\mathrm{d}u}{(u^2-1)^{1/2}}\,\frac{\mathrm{d}}{\mathrm{d}u}f(|b|\,u)\,, \\
x' &= x + P\,\frac{\cos\bar{\alpha}}{(\sin^2\bar{\beta} - \cos^2\bar{\alpha})^{1/2}}\,, \\
y' &= y + P\,\frac{\cos\bar{\beta}}{(\sin^2\bar{\beta} - \cos^2\bar{\alpha})^{1/2}}\,.
\end{aligned}\right\} \tag{2.6}$$

The last two equations for the position coordinates x' and y' of the particle in the channel are easily derived from Fig. 2.

In order to linearize these equations we assume the angles $\bar{\alpha}$ and $\bar{\beta}$ to be very close to $\pi/2$; afterwards, we expand with respect to r supposed to be small and obtain

$$\left.\begin{aligned}
\alpha' &= \alpha + \frac{R}{E}\int_0^{2\pi}\mathrm{d}\theta\varrho(\theta)\,(\operatorname{sgn}\sin\theta)\int_1^{\infty}\frac{\mathrm{d}u}{(u^2-1)^{1/2}}\,\frac{\mathrm{d}}{\mathrm{d}u}f(Ru) - \frac{1}{E}\int_0^{2\pi}\mathrm{d}\theta\varrho(\theta)\times \\
&\quad\times(\operatorname{sgn}\sin\theta)\,r\cos(\theta-\psi)\int_1^{\infty}\frac{\mathrm{d}u}{(u^2-1)^{1/2}}\,\frac{\mathrm{d}}{\mathrm{d}u}\left[u\,\frac{\mathrm{d}}{\mathrm{d}u}f(Ru)\right], \\
x' &= x + P\alpha
\end{aligned}\right\} \tag{2.7}$$

and analogous relations for β and y.[4])

With the distribution function of the potential source

$$\varrho(\theta) = \delta(\theta) + \delta(\theta - \pi) \tag{2.8}$$

[4]) The appearance of the factor $r\cos(\theta - \psi)$ by linearization in the present context means assuming a harmonic interaction potential. This approximation may be good enough for those particles which are moving close to the channel axis. It is well known from ion optics that transfer matrix technique methods require harmonic potentials.

we obtain

$$X' = (I + \Delta_1)\, X\,, \tag{2.9}$$

where

$$X = \begin{pmatrix} X^1 \\ X^2 \end{pmatrix}, \quad X^1 = \begin{pmatrix} P\alpha \\ P\beta \end{pmatrix}, \quad X^2 = \begin{pmatrix} x \\ y \end{pmatrix}, \tag{2.9'}$$

$$\Delta_1 = \begin{pmatrix} -4Q & 0 & -4Q & 0 \\ -4Q & 0 & -4Q & 0 \\ 1 & 0 & 0 & 0 \\ 0 & 1 & 0 & 0 \end{pmatrix}, \qquad Q = \frac{P}{2E} \int_1^\infty \frac{\mathrm{d}u}{(u^2-1)^{1/2}} \frac{\mathrm{d}}{\mathrm{d}u}\left[u \frac{\mathrm{d}}{\mathrm{d}u} f(Ru)\right], \tag{2.10}$$

and I the 4×4 unit matrix. With the function

$$\varrho(\theta) = \delta\left(\theta - \frac{\pi}{2}\right) + \delta\left(\theta - \frac{3\pi}{2}\right) \tag{2.11}$$

Δ_1 in (2.9) is substituted by Δ_2,

$$\Delta_2 = \begin{pmatrix} 0 & -4Q & 0 & -4Q \\ 0 & -4Q & 0 & -4Q \\ 1 & 0 & 0 & 0 \\ 0 & 1 & 0 & 0 \end{pmatrix}. \tag{2.12}$$

We denote the group of the two neighbouring rings by n and obtain the recurrence relation

$$X_n = (I + \Delta_1)\,(I + \Delta_2)\, X_{n-1}\,. \tag{2.13}$$

The matrix $(I + \Delta_1)\,(I + \Delta_2)$ has a double eigenvalue equal to unity; the remaining other two are given by

$$\lambda_{1,2} = 1 + 8\left[Q^2 - Q \pm \sqrt{(Q^2 - Q)^2 + \tfrac{1}{4}(Q^2 - Q)}\right]. \tag{2.14}$$

Hence it results the condition of stability: for $0 < Q < 1$ the trajectory is stable, for the other value of Q it is unstable. The condition $Q = 1$ gives the minimum critical hyperchanneling energy (see Section 3).

In order to solve the equation of the stable trajectory it is necessary to know the n-th power of the product $(I + \Delta_1)\,(I + \Delta_2)$. Since $0 < Q < 1$ the calculation is complicated by small quantities, so that we use the following approximation. The eigenvalues of the matrices Δ_1 and Δ_2 are of order $\sqrt{Q}$. With an error of order Q we neglect the product $\Delta_1\Delta_2$ with respect to Δ_1 and Δ_2. Indeed, the matrix $I + \Delta_1 + \Delta_2$ has a double eigenvalue equal to unity and the remaining other two are given by

$$\lambda_{1,2} = 1 - 4Q \pm 4\sqrt{Q^2 - Q}\,. \tag{2.15}$$

The stability condition is preserved, but the determinant of the matrix $I + \Delta_1 + \Delta_2$ is different from unity. In order to satisfy Liouville's theorem we normalize the eigenvalues of this matrix to unity. The matrix A obtained in this way can

be easily raised to the n-th power:

$$A^n = \begin{Bmatrix} \frac{|\lambda|^{1/2}}{q}(1-4Qt)\sin n\varphi + & -\frac{4|\lambda|^{1/2}\,Qt}{q}\sin n\varphi \\ +\frac{1}{q|\lambda|}(1+4Qt)\sin(n-1)\varphi & \\ \frac{2|\lambda|^{1/2}}{q}\sin n\varphi & \frac{|\lambda|^{1/2}}{q}\sin n\varphi + \\ & +\frac{1}{q|\lambda|}(1+4Qt)\sin(n-1)\varphi \end{Bmatrix} \tag{2.16}$$

where

$$\left.\begin{aligned} q &= 4[Q(1-Q)]^{1/2}\,, & |\lambda| &= (1+8Q)^{1/2}\,, \\ \sin\varphi &= \frac{q}{|\lambda|}\,, & t &= \begin{pmatrix} 1 & 1 \\ 1 & 1 \end{pmatrix}. \end{aligned}\right\} \tag{2.17}$$

The condition $X_0 = 0$ implies $X_n = 0$ for every n. It gives a selection of hyperchanneled particles whose trajectories coincide with the axis of the channel.

As in the two-dimensional case [7], the influence of the temperature is taken into account by averaging the equations of motion with respect to the thermal vibrations of the lattice atoms. We assume these vibrations are much smaller than the lattice constant. Vibrations in angle θ and vibrations parallel to the channel axis are neglected. For the latter vibrations the same considerations are valid as in the two-dimensional case [7]. For those particles which move in the neighbourhood of the channel axis we have estimates by geometrical reasons that the effect of vibrations in θ is a second-order one compared to radial vibrations. The radial vibrations with respect to ξ lead us to the substitution of Q by $\langle Q\rangle$ with the expansion

$$\langle Q\rangle = Q + Q_1\langle\xi^2\rangle/R^2\,, \tag{2.18}$$

where

$$Q_1 = \frac{P}{4E}\int_1^\infty \frac{\mathrm{d}u}{(u^2-1)^{1/2}}\frac{\mathrm{d}}{\mathrm{d}u}\left[u\frac{\mathrm{d}}{\mathrm{d}u}u^2\frac{\mathrm{d}^2}{\mathrm{d}u^2}f(Ru)\right] \tag{2.19}$$

and the brackets $\langle\cdots\rangle$ denote the thermal mean value.

Let us assume that a particle enters the centre of the ring, so that $X_0^2 = 0$. We require the particle to be confined inside the effectively open channel; so the largest value of x_n and y_n for any n, will be τR, where τ is a subunitary factor which depends on the range of the interaction between projectile and target atoms. This range is essentially the Thomas-Fermi screening length which is of order 0.2 Å. The atom-projectile distances are of order 2 Å so that τ may be taken in the following as equal to 0.9.

The above-mentioned condition gives the critical angles

$$\alpha_c^0 = \beta_c^0 = \tau\frac{R}{2P}\frac{q}{|\lambda|^{1/2}}. \tag{2.20}$$

The temperature dependent critical angles are

$$\alpha_c = \beta_c = \tau \frac{R}{2P} \frac{\langle q \rangle}{|\langle \lambda \rangle|^{1/2}} \left\{ 1 - \left[\frac{\langle \xi^2 \rangle}{R^2} \right]^{1/2} \right\}, \tag{2.21}$$

where the radius of the channel was estimated at $\tau R\{1 - [\langle \xi^2 \rangle / R^2]^{1/2}\}$. It is easily to see that the critical angles are decreasing with increasing the energy and temperature.

3. Discussion

The aim of this section is to give some illustrative results. So we can restrict to the Coulomb potential $Z_1 Z_2 e^2/r$ where Z_1 and Z_2 are the charge numbers of the moving particle and of the crystal atoms, respectively, e is the electron charge. It is also possible to use another suitable potential. The quantities Q and Q_1 are not so sensitive to the special form of the chosen potential. If we take $Z_1 \approx 1$, $Z_2 \approx 10$, the energy, $E \approx 1$ MeV, then the quantities Q and Q_1 are of order 10^{-3}. We see that the stability condition for hyperchanneling is fulfilled. The minimum critical hyperchanneling energy resulting from $Q = 1$ is of order 1 to 10 keV. Such a critical energy has not been considered in the literature so far. The critical angle results to be of order 10^{-2} rad and smaller. Both its order of magnitude and slight dependence on the temperature agree well with the experiments [4, 5]. As concerns the energy loss due to the collisions of the moving particle with the atomic rings — the electronic stopping is not a subject in our paper — it is necessary to know the energy loss produced by the n-th collision, which is

$$\Delta E_n = E_{n-1}[(\Delta\alpha_n)^2 + (\Delta\beta_n)^2], \tag{3.1}$$

where $\Delta\alpha_n = \alpha' - \alpha$, $\Delta\beta_n = \beta' - \beta$ are given by (2.7) or more exactly obtainable from (2.13). It is possible, by considering n to be a continuum variable, to obtain the average stopping power $\mathrm{d}E/\mathrm{d}n$. It is easily to see that the total stopping power can be regarded as a sum of the stopping power for two planar channels [7]:

$$\frac{\mathrm{d}E}{\mathrm{d}n} = -\frac{16E^2}{E(n)} \left\langle Q^2 \frac{x(n)^2 + y(n)^2}{P} \right\rangle_n, \tag{3.2}$$

where the brackets denote the mean value over a small width covering the actual value of n. Under the above mentioned conditions we obtain an energy loss of order 10^{-5} MeV/μm. This value is the atomic stopping power and obviously is much smaller than the experimental values ($\approx 10^{-2}$ MeV/μm), due to the fact that we have entirely neglected in our calculation the electronic stopping power.

The linearization of the equations of motions is well justified. Using the Coulomb potential it can be shown that the linearization is valid over almost 0.9 of the channel width with a relative error which does not exceed 10%.

The expression for the critical angle shows a good behaviour with energy and temperature as mentioned before. The critical angles contain generally the factor $(Q - Q^2)^{1/2}$. The dependence of the critical angles upon the energy, in the high energy limit, is concentrated mainly in Q (because Q^2 can be generally neglected as compared to Q for large energies); in this case our relation for hyperchanneling angles goes as $E^{-1/2}$ as predicte by Lindhard for ordinary channeling. However, the magnitude of our hyperchanneling critical angle is of course less than Lindhard's critical angle of ordinary axial channeling.

Each given channel requires a specific mathematical treatment. The present calculation has been limited to a special case of an axial channel defined by two potential source density functions (2.8) and (2.11). Our intention has not been to give an extensive solution of the channeling phenomena but rather to show how the transfer matrix technique can be used in working out the hyperchanneling trajectories.

Acknowledgement

The authors are deeply indebted to the referee for his careful reading of the manuscript and many valuable suggestions.

References

[1] M. T. Robinson and O. S. Oen, Phys. Rev. **132**, 2385 (1963).
[2] G. Lehmann and G. Leibfried, J. appl. Phys. **34**, 2821 (1963).
[3] J. Lindhard, Mat.-Fys. Medd. Dan. Vid. Selsk. **34**, No. 14 (1965).
[4] F. H. Eisen, Phys. Letters (Netherlands) **23**, 401 (1966).
[5] B. R. Appleton, C. D. Moak, T. S. Noggle, and J. H. Barret, Phys. Rev. Letters **28**, 1307 (1972).
[6] A. Corciovei, M. Apostol, and D. Mihalache, Phys. Letters **44A**, 259 (1973).
[7] A. Corciovei, M. Apostol, and D. Mihalache, Rev. Roum. Phys. **18**, 557 (1973).

(Received October 14, 1974)